Electronic Supplementary Information (ESI)

Dual activity inhibition of Threonine aspartase 1 by a single bisphosphate ligand

Alexander Höing,[a] Robin Struth,[b], Christine Beuck,[c] Neda Rafieiolhosseini,[d] Daniel Hoffmann,[d] Roland H. Stauber,[e] Peter Bayer,[c] Jochen Niemeyer,*[b] and Shirley K. Knauer*[a]

[a] *A. Höing, Prof. Dr. S.K. Knauer*
Molecular Biology II, Center of Medical Biotechnology (ZMB)/Center for Nanointegration Duisburg-Essen (CENIDE), University of Duisburg-Essen, Universitätsstrasse 5, 45141 Essen, Germany; E-mail: shirley.knauer@uni-due.de
[b] *R. Struth, Prof. Dr. J. Niemeyer*
Organic Chemistry, Center for Nanointegration Duisburg-Essen (CENIDE), University of Duisburg-Essen, Universitätsstrasse 7, 45141 Essen, Germany Germany; E-mail: jochen.niemeyer@uni-due.de
[c] *Dr. C. Beuck, Prof. Dr. P. Bayer*
Structural and Medicinal Biochemistry, Center for Medical Biotechnology (ZMB), University of Duisburg-Essen, Universitätsstrasse 5, 45141 Essen, Germany
[d] *N. Rafieiolhosseini, Prof. Dr. D. Hoffmann*
Bioinformatics and Computational Biophysics, Center for Medical Biotechnology (ZMB), University of Duisburg-Essen, Universitätsstrasse 5, 45141 Essen, Germany
[e] *Prof. Dr. R.H. Stauber*
Molecular and Cellular Oncology/ENT, University Medical Center Mainz (UMM), Langenbeckstrasse 1, 55101 Mainz, Germany

Content

List of Figures and Tables

Figures

Tables

Taspase 1 activation

Taspase 1 has to undergo a distinct, multistep activation process to execute its pathobiological cleavage activity.

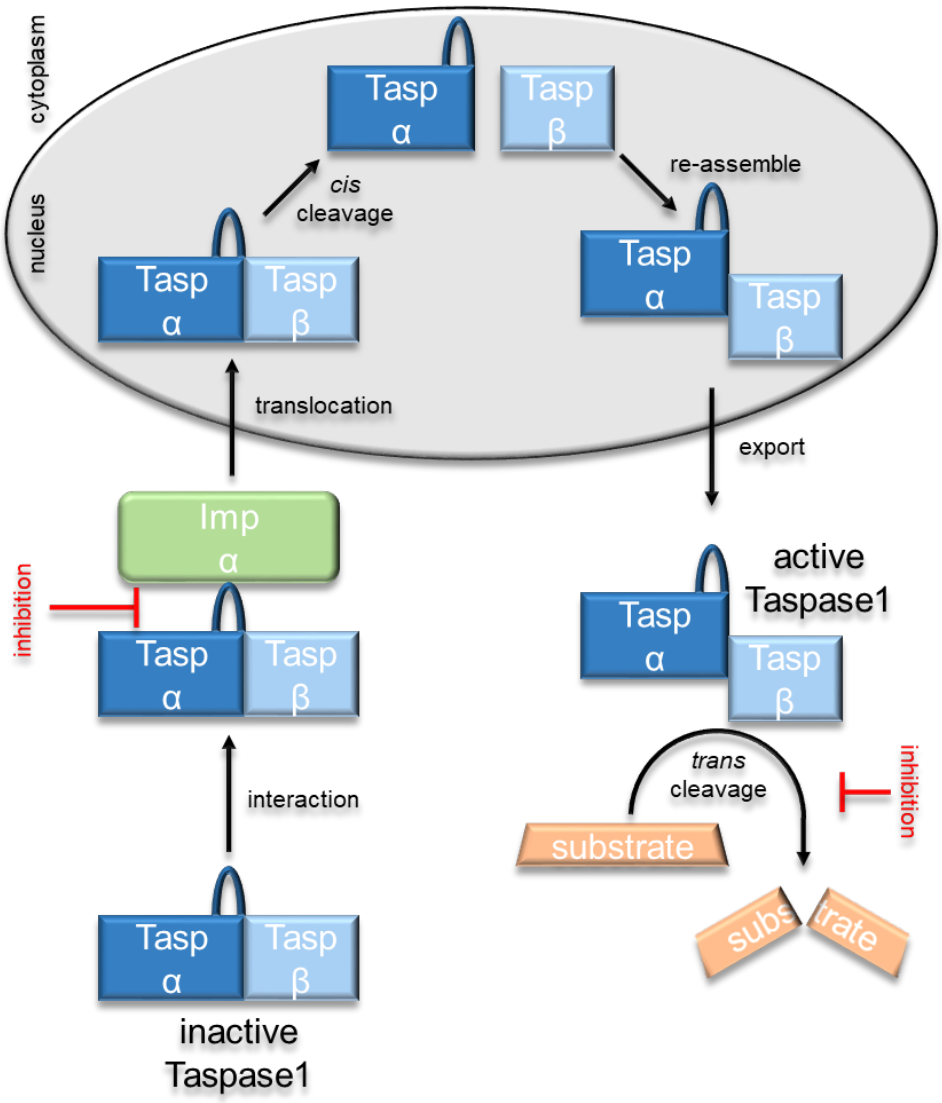

Figure S1. Activation process of Taspase 1. The activation involves the protein-protein interaction with Importin α and the conversion of Taspase 1 from an inactive monomer to an active heterodimer through *cis* cleavage. Inhibition mechanisms are indicated.

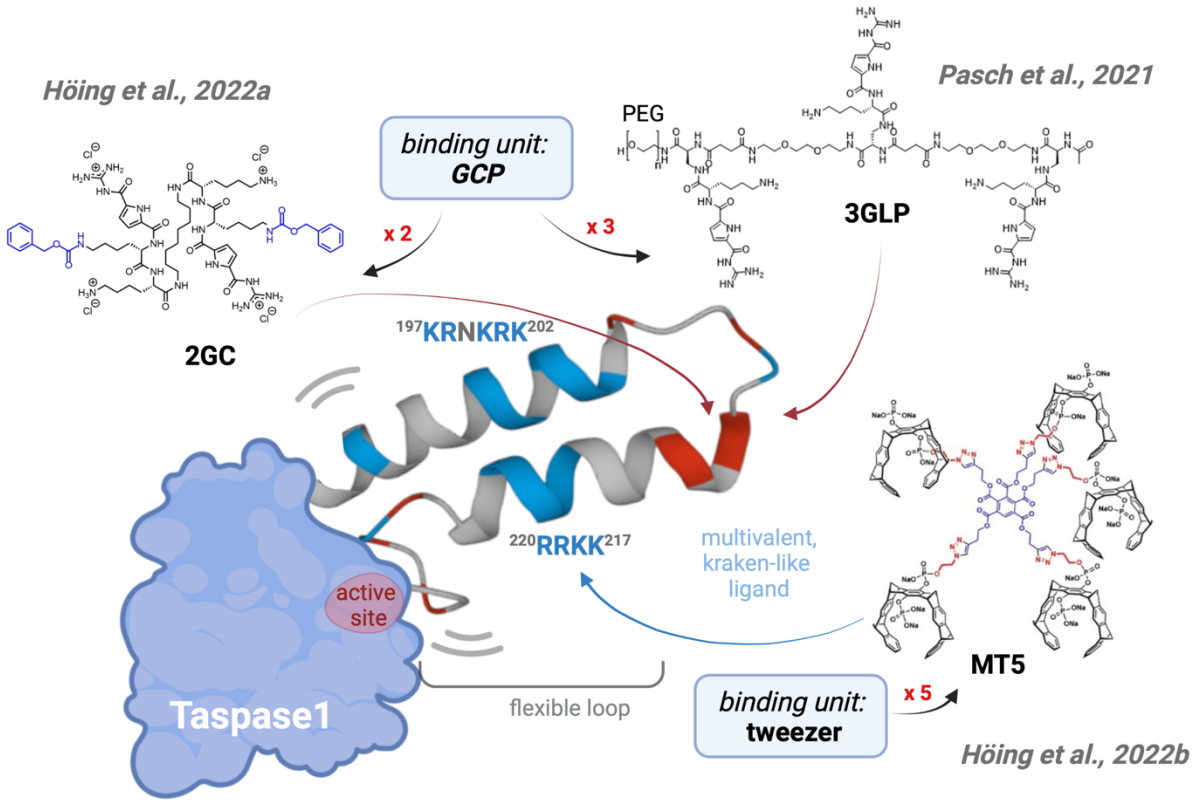

Figure S2. Supramolecular targeting approaches for Taspase 1. Compounds **2GC** and **3GLP** harbor 2 or 3 GCP units, respectively, to address acidic amino acid clusters (red) on the surface-exposed Taspase 1 loop. Supramolecular ligand **MT5** is a multivalent construct build of 5 molecular tweezer units addressing the two basic amino acid clusters (blue) constituting Taspase 1's NLS on the loop structure (amino acids indicated). For more details, see text in the main manuscript. Created with Biorender.com.

Table S1. Supramolecular targeting approaches for Taspase 1.

Year	Inhibitor	Binding unit/ composition	Targeted residues	Inhibition	Solvent	Reference
2021	**3GLP**	GCP (3x) + PEG on a macromolecular scaffold	acidic (Glu, Asp)	Importin binding: **first effects at 10 µM** Proteolytic activity: **no** Cellular toxicity: **no** Cell permeability: n.d.	H_2O	Pasch P., Höing A., Ueclue S., Killa M., Voskuhl J., Knauer S.K., Hartmann L. **PEGylated sequence-controlled macromolecules using supramolecular binding to target the Taspase1/Importin α interaction.** *Chemical Communications*, 57:3091-3094.
2022	**2GC**	GCP (2x)	acidic (Glu, Asp)	Importin binding: **IC_{50} 34 µM** Proteolytic activity: **first effects at 400 µM** Cellular toxicity: **EC_{50} 40-70 µM** Cell permeability: **yes**	DMSO (1%)	Höing A., Zimmermann A., Moews L., Killa M., Heimann M., Hensel A., Voskuhl J., Knauer S.K. **A bivalent supramolecular GCP-ligand enables blocking of the Taspase1/Importin α interaction.** *ChemMedChem*, doi.org/10.1002/cmdc.202100640.
2022	**MT1-MT5**	molecular tweezer (mono- to pentavalent)	basic (Lys, Arg)	For **MT5**: Importin: **first effects at 2 µM** Proteolytic: **IC_{50} ~2 µM** Cellular toxicity: **n.d.** Cell permeability: **n.d./no**	DMSO (3%)	Höing A., Kirupakaran A., Beuck C., Pörschke M., Niemeyer F.C., Seiler T., Hartmann L., Bayer P., Schrader T., Knauer S.K. **Recognition of a flexible protein loop in Taspase 1 by multivalent supramolecular tweezers.** *Biomacromolecules*, doi:10.1021/ acs.biomac.2c00652.

n.d., not done.

Chemical Assays

Compound synthesis and purification

Ligands **1d/e/f** and **11d/e/f** were prepared according to literature procedures.[1-3] For all experiments, the ligands were used as stock solutions in DMSO (analytical grade), which were prepared by dissolving the solid ligands in an appropriate amount of DMSO to reach a concentration of 100 mM. Aliquots of these stock solutions were used to reach the desired concentrations of **1d/e/f** and **11d/e/f** in further experiments.

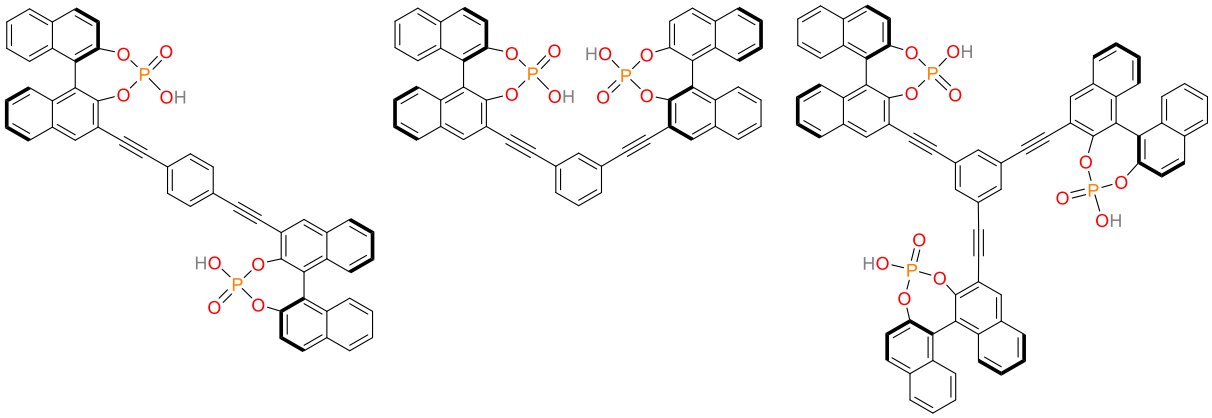

(*R*,*R*)-**1d**

Chemical Formula: $C_{50}H_{28}O_8P_2$
Molecular Weight: 818,71

(*R*,*R*)-**1e**

Chemical Formula: $C_{50}H_{28}O_8P_2$
Molecular Weight: 818,71

(*R*,*R*,*R*)-**1f**

Chemical Formula: $C_{72}H_{39}O_{12}P_3$
Molecular Weight: 1189,01

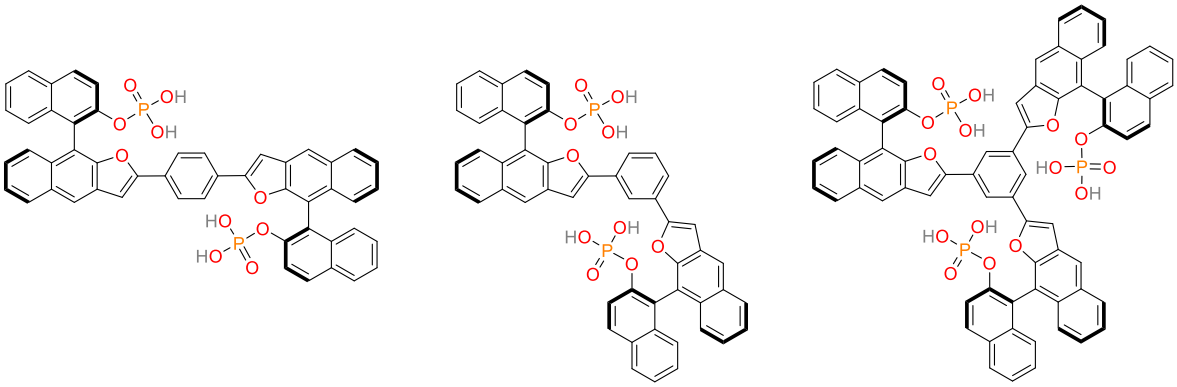

(*R*,*R*)-**11d**

Chemical Formula: $C_{50}H_{32}O_{10}P_2$
Molecular Weight: 854,7435

(*R*,*R*)-**11e**

Chemical Formula: $C_{50}H_{32}O_{10}P_2$
Molecular Weight: 854,7435

(*R*,*R*,*R*)-**11f**

Chemical Formula: $C_{72}H_{45}O_{15}P_3$
Molecular Weight: 1243,0583

Figure S3. Chemical structures of phosphate-based ligands (*all-R*)-**1d/e/f** and (*all-R*)-**11d/e/f**. The ligands were exclusively used as the (*R,R*)- and (*R,R,R*)-isomers respectively (no further stereodescriptors are given in the text).

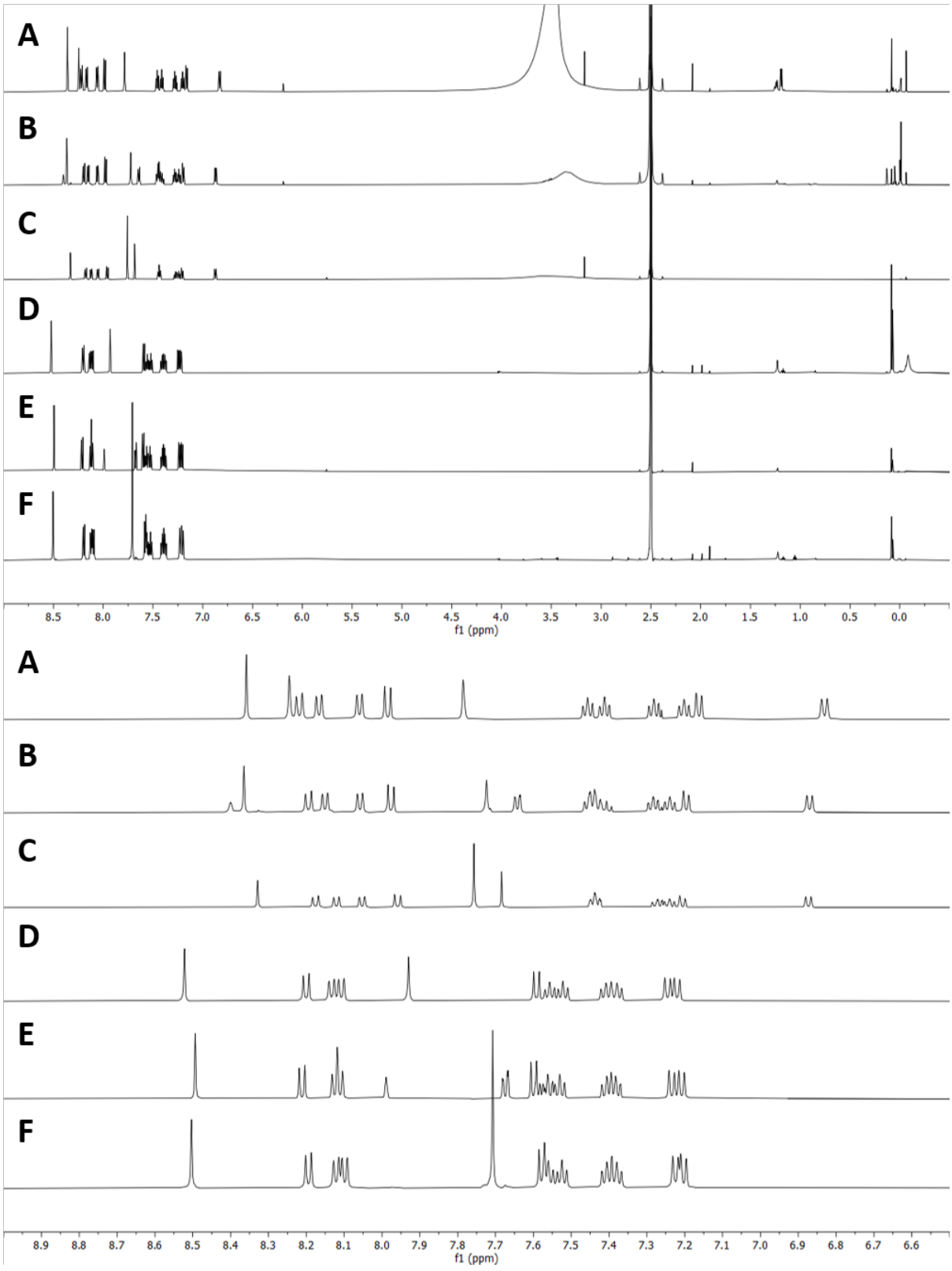

Figure S4. ^{1}H NMR-spectra of all phosphate-based ligands. Top: Full spectra, bottom: aromatic region only. A) (*R*,*R*)-**1d**, B) (*R*,*R*)-**1e**, C) (*R*,*R*,*R*)-**1f**, D) (*R*,*R*)-**11d**, E) (*R*,*R*)-**11e**, F) (*R*,*R*,*R*)-**11f**, (all: [D_6]-DMSO, 600 MHz, 298 K, also see ref. 1-3).

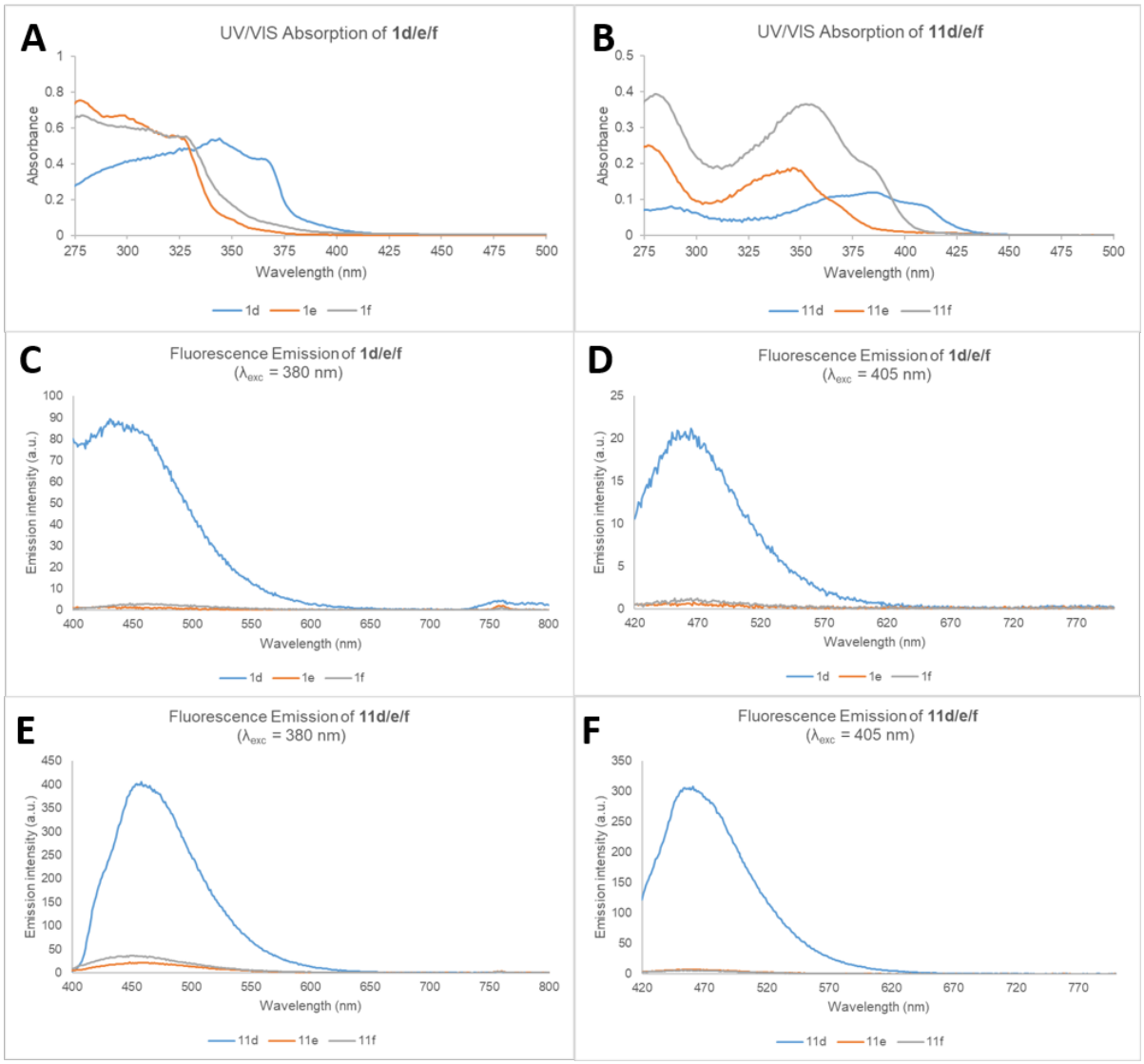

Figure S5. Absorption and emission spectra of phosphate-based ligands. A/B) Absorption spectra of **1d/e/f** and **11d/e/f**. C/D) Emission spectra of **1d/e/f** with λ_{exc} =380/405 nm. E/F) Emission spectra of **11d/e/f** with λ_{exc} =380/405 nm. **11d** has superior emission intensity at the excitation wavelength used for fluorescence anisotropy (380 nm, C) and confocal laser scanning microscopy (405 nm, D) (all: H_2O/DMSO = 95/5, 10 µM).

Table S2. Quantum yields and fluorescence lifetimes of **1d/e/f** and **11d/e/f**.

	Quantum yields[a] Φ	Lifetime components τ [ns] (relative amplitudes in %)[b]
1d	0.70	1.2 (88), 0.4 (12)
1e	0.28	5.4 (72), 2.7 (28)
1f	0.21	5.9 (45), 3.9 (55)
11d	0.28	1.9 (94), 0.8 (6)
11e	0.37	7.5 (60), 4.7 (40)
11f	0.23	8.2 (44), 4.6 (56)

All values measured in in DMF/water (99/1). [a] 1 µM solutions, λ_{exc} = 305 nm; [b] 1 µM solutions, λ_{exc} = 405 nm. Data taken from Octa-Smolin et al., 2017.[2]

Computational studies

Modelling

To compute the affinity map of Taspase 1 with **11d**, we proceeded as follows:

The initial structure of the ligands was obtained using Maestro Schrodinger V.3.0.[4] Van der Waals radii and partial charges of ligand atoms (MMFF94_CHARGES) were added automatically by OpenBabel V.3.1.0.[5] Values are provided in Table S3. To specify the ligands' protonation states which are similar to the protonation state of naphthyl phosphate, there were no experimentally reported value in the literature. Assuming that the protonation state of naphthyl phosphate at pH 7.0 is close to the one of methyl phosphate for which the experimental pK_a values are reported in the literature (pK_{a1} = 1.5, pK_{a2} = 6.3),[6] we used models of our ligands with doubly deprotonated phosphate groups in our calculations as exemplary depicted for **11d**.

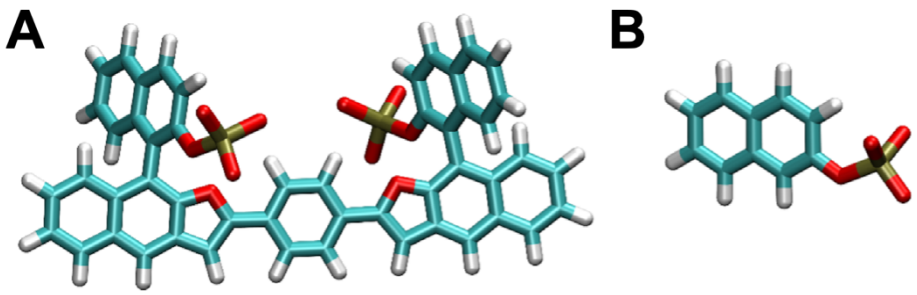

Figure S6. Ligand **11d** with deprotonated phosphate groups (A) and naphthyl phosphate (B).

The model of Taspase 1 that we used in this study was previously generated in the group of Prof. Peter Bayer.[7] This model contained a disordered region comprising aa residues 1 to 39 that was removed for modelling. Charges, van der Waals radii and missing hydrogen atoms were added by PDB2PQR web service v3.1.0 at pH 7.0 with the Amber force field option.[8]

Energy grid

To calculate the electrostatic field of Taspase 1, we solved the nonlinear Poisson-Boltzmann equation with APBS[7] with ionic concentrations of 0.150 mol/L NaCl and relative dielectric permittivities $\epsilon_r^{protein} = 2$ and $\epsilon_r^{water} = 79$. Epitopsy[9] was used to scan the Taspase 1 environment with naphthyl-phosphate using a grid resolution of 0.4 Å, pH 7.0, and a temperature of 298K. Here the reason to use naphthyl phosphate instead of the whole ligand is that Epitopsy assumes the protein and the ligand are rigid structures. Therefore, if the whole ligand with all its degrees of freedom and flexibility is used, the assumption will be far from reality.

Note that in the above-mentioned approach only the interactions of individual naphthyl phosphate with Taspase 1 are obtained. To model the interactions of Taspase 1 with the full **11d** ligand, we combined this approach with further interactions as described.[10]

Table S3. Names, coordinates, partial charges, and Van der Waals radii of **11d** ligand atoms.

	X	Y	Z	Charge	Radius
O	4.513	6.518	-2.081	-1.0333	1.52
O	2.676	4.543	-1.084	-1.0333	1.52
C	5.782	5.463	2.312	-0.15	1.7
C	5.309	5.248	1.014	-0.15	1.7
C	5.906	4.275	0.187	0.0825	1.7
C	6.981	3.525	0.681	-0.15	1.7
C	7.463	3.733	1.982	0	1.7
C	6.858	4.712	2.806	0	1.7
C	8.54	2.981	2.477	-0.15	1.7
C	9.011	3.198	3.775	-0.15	1.7
C	8.413	4.165	4.587	-0.15	1.7
C	7.34	4.921	4.107	-0.15	1.7
O	5.486	4.027	-1.078	-0.3537	1.52
P	4.191	4.824	-1.885	1.3712	1.8
O	4.089	4.202	-3.303	-1.0333	1.52
H	5.307	6.216	2.929	0.15	1.1
H	4.478	5.846	0.669	0.15	1.1
H	9.017	2.227	1.861	0.15	1.1
H	9.842	2.615	4.152	0.15	1.1
H	8.782	4.329	5.591	0.15	1.1
H	6.888	5.666	4.751	0.15	1.1
H	7.44	2.776	0.045	0.15	1.1

Bead-Spring model of the ligand

We have previously developed a coarse-grained bead-spring[11-13] model of a luminescent ligand.[10] We applied the same approach to ligand **11d** such that each of the five chemical groups of the ligand is represented by one bead (see Figure 5B). Each bead is located at the geometric center of the corresponding chemical group. Neighboring beads interact with each other through a harmonic potential. Given the symmetry of ligand **11d**, we consider two sets of spring parameters. We assigned an equilibrium length of 4.5 Å and a spring constant of 25 $k_BT/Å^2$ to the spring connecting the first bead to the second one. The spring connecting the second bead to the third one, has the same spring constant but a different equilibrium length of 7 Å. These parameters are selected such that they keep the beads at reasonable distances. Overlaps between non-bonded beads are avoided by repelling potentials. For more details about the model we refer the reader to our published work.[10] For simplicity, we do not include the angles in our model. Instead, we opt to filter out the final structures obtained from our simulations and only keep those with reasonable angles.

Simulated Annealing Monte Carlo (SAMC) simulations

We did 4000 runs of SAMC to identify the globally optimal configuration of **11d** around Taspase 1 as previously described.[11] At the beginning of each run, we put the central bead at a random grid position within a volume layer around the protein. The thickness of the layer corresponded to the distance between the central bead and the last bead in the chain. Its volume is about 173 nm^3, so that the 4000 initial positions sample the layer at a density of about 23 per nm^3.

Results obtained from our SAMC runs (Figure S7A) suggest that the most likely binding site is in the region around the NLS loop of protein Taspase 1. This binding site is in the positively charged region of the protein surface (Figure S7B).

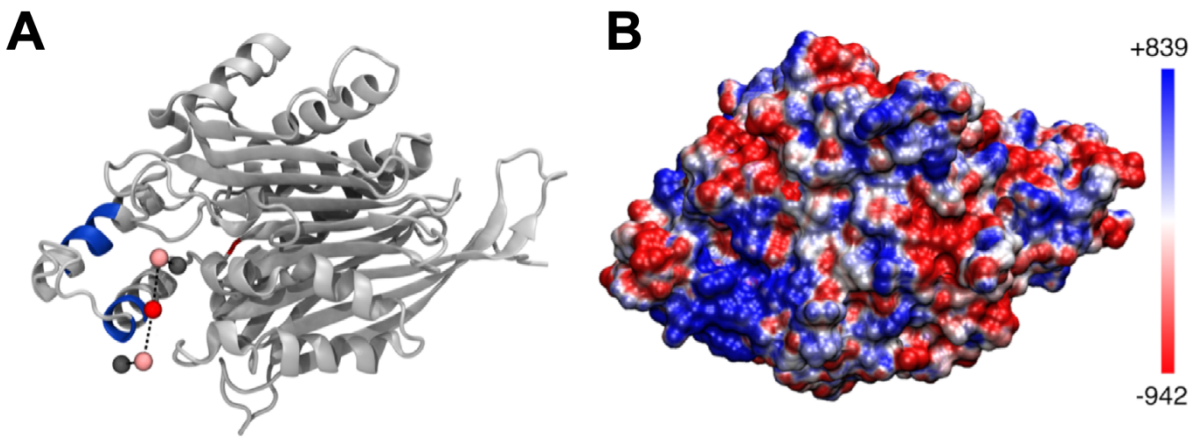

Figure S7. A) The most probable binding position of **11d** obtained from SAMC simulations. The ligand is represented as a bead-spring model where each colored bead indicates the respective group. Blue, bipartite NLS. B) The electrostatic potential on the surface of Taspase 1. The coloring method is based on the surface potential from dark red (most negative) to dark blue (most positive). The values in the color bar are in units of $k_BT/|e|$.

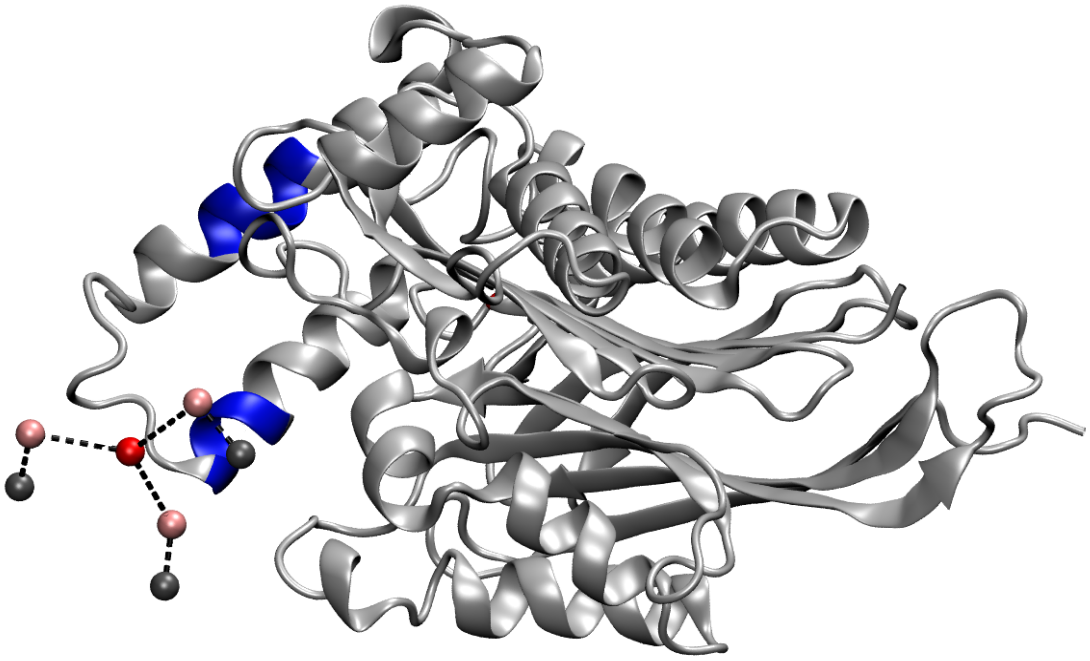

Figure S8. The most probable binding position of **11f** obtained from SAMC simulations. The ligand is represented as a bead-spring model where each colored bead indicates the respective group. Blue, bipartite NLS.

Biological Assays

Cloning

The plasmids for inactive mutant Taspase 1D233/T234A,[14, 15] wild type Taspase 1,[16] the Taspase 1 $loop_{178-233}$[7] and GST-PreScn-Importin α[17] were previously described. The plasmid for cleavage probe GST-$MLL_{2700-2850}$-GFP-His was generated by DNA assembly. The backbone was generated by XhoI/NdeI digestion of pET22b-Taspase 1-His.[16] The fragments for assembly were amplified by PCR with overlaps introduced by adequate primer pairs (Table S4). 15 fmol backbone was mixed with at least 5-fold excess of each insert, mixed with the using the NEBuilder® HiFi DNA Assembly Master Mix (New England Biolabs) and incubated at 50 °C for 30 min. The resulting plasmid was directly transfected into competent *E. coli* NEB-10ß (New England Biolabs). The sequence of the plasmid was validated by sequence analysis (LGC Genomics).

Table S4. Plasmids and primer pairs used for NEB assembly.

Fragment	Source	Forward primer	Reverse primer
GST	pC3-GST-USF2-GFP[16]	ctttaagaaggagatatacaATGTCCCCTATACTAGGTTATTG	CAGATCCGATTTTGGAGG
MLL2700-2850	JH1117 WT-MLL[18]	atcctccaaaatcggatctgTCTTCAGGTGGAGAGGAAC	agctcctcgcccttgctagcGTCATCACTGTTGTTATTGTC
GFP	pC3-GST-USF2-GFP[16]	GCTAGCAAGGGCGAGGAG	agtggtggtggtggtggtgc*tcgag*CTTGTACAGCTCGTCCATGC

Expression and purification of recombinant proteins

pET22b-Taspase $1_{D233A/T234}$-His, pET22b-WT_Taspase 1-His and pET41-GST-PreScn-Importin α were expressed and purified as previously described (Fig. S7).[17] [15]N-labelled Taspase 1 $loop_{178-233}$ for NMR titrations was expressed and purified as described previously. pET22b-GST-$MLL_{2700-2850}$-GFP-His was expressed in *E. coli* BL21 (DE3). The cells were lysed using sonication and treated with lysozyme. Cell debris and insoluble fragments were removed by centrifugation and filtration. The protein was purified using a tandem affinity approach utilizing the N-terminal GST-tag and the C-terminal His-Tag. The GFP-tag allowed to track protein integrity during purification. The soluble fraction was loaded onto a glutathione sepharose GSTrap 4B column (Cytiva). Following glutathione elution, the GST-containing fractions were pooled and loaded onto a HisTrap column (Cytiva). Following imidazole elution, the His-containing fractions were pooled, and the buffer was exchanged for Taspase 1 kinetic buffer (10 % sucrose, 50 µM $NaH2PO_4$, pH 7.4) using a Vivaspin concentrator with a 30 kDa molecular weight cut-off. The protein was frozen in liquid nitrogen and stored at -20 °C. Purity was verified using SDS-PAGE and immunoblotting.

SDS-PAGE and immunoblotting

We used the standard protocols for SDS-PAGE according to Laemmli and for immunoblotting according to Towbin.[19, 20] Briefly, for SDS-PAGE, Tris-glycine gels with 12.5 % or 10 % (v/v) acrylamide in the stacking gel and 4 % (v/v) acrylamide in the separating gel were prepared accordingly. For subsequent electrophoresis, we used the TetraCell system (BioRad) set to 200 V for 45 min. Proteins were then transferred to a protein-binding nitrocellulose membrane using a wet blot tank (Peqlab) set to 360 mA for 90 min at 4 °C. The membrane was first reversibly stained with Ponceau S (AppliChem) and the membrane cut between the protein bands according to the Spectra Multicolor Broad Range Protein Ladder (Thermo Fisher) to analyze proteins from the same sample. Free binding sites were blocked with 5 % (w/v) powdered milk (Carl Roth) in Tris-buffered saline with Tween-20 (Carl Roth) (TBST) for 60 min at room temperature. After that, membranes were incubated with the respective primary antibodies rabbit anti-Taspase 1 1:2000 (sc-85945, Santa Cruz) or mouse anti-Karyopherinα2 1:1000 (sc-55538, Santa Cruz) in 5% (w/v) powdered milk in TBST over night at 4 °C. Unbound antibodies were removed by three washing steps with TBST. Membranes were incubated with the respective secondary antibodies donkey anti-rabbit HPR-coupled 1:10000 (NA934, GE Healthcare) or sheep anti-mouse HPR-coupled 1:10000 (NXA931, GE Healthcare) in 5% (w/v) powdered milk with TBST for 1 h at room temperature. Unbound antibodies were removed by four washing steps in TBST. For the detection of chemiluminescence, we used the Pierce ECL Plus Western Blotting Substrate (Thermo Fisher) and the Chemidoc Imaging System (BioRad). Automatic exposure time was chosen to avoid overexposure and to ensure equal maximum signal intensity in all blots. Densitometric quantification of the signals was performed using Fiji.[21] If necessary, the signal of Taspase 1 in the eluted fraction was corrected for Taspase 1 bound to the column without Importin α. To correct possible loading differences, the signal of Taspase 1 in the eluted fraction was normalized to the signal of Importin α in the eluted fractions. The data was evaluated using Origin2019 (OriginLab). Homoscedasticity of the samples was tested by Levene-test. Depending on the result, significances were determined by t-test or Welch-t-test to correct differences in the variance of the samples.

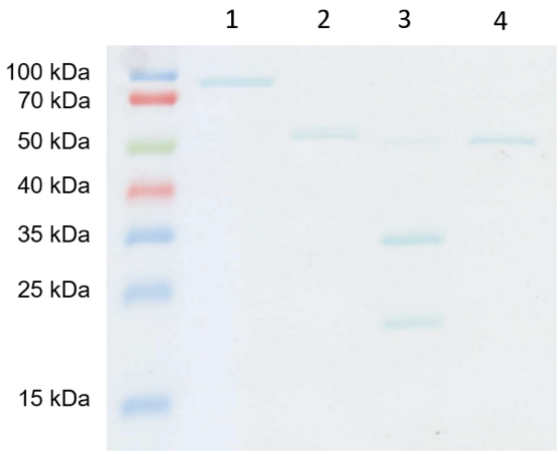

Figure S9. Coomassie-stained polyacrylamide gel of recombinantly expressed proteins. Marker :Spectra™ Multicolor Broad Range Protein Ladder (positions of molecular mass standard in kDa are indicated on the left). GST-Importin α (82 kDa, lane 1); Importin α (57 kDa, lane 2); wild-type Taspase 1-His, partially autocatalytically processed into the subunits α and β (45 kDa, 25 kDa, 20 kDa, lane 3); catalytically inactive mutant Taspase $1_{D233A/T234}$-His (45 kDa).

Pull-down assay

For the pull-down assay, we used Dulbecco's Phosphate Buffered Saline (Sigma-Aldrich) containing 0.1 % (v/v) Triton X-100 (Carl Roth) and 1 mM DTT (Carl Roth) (PBST). Incubation steps were carried out at 4 °C to avoid protein degradation. Centrifugation steps were carried out at 500 x G if not stated otherwise. Samples taken for later analysis were mixed with 5x sample buffer[19] and heated to 95 °C for 5 min. 50 µM slurry of Glutathione Sepharose 4B (Merck) was transferred to a Spin Column (IBA Lifescience) and equilibrated with 500 µL PBST followed by centrifugation. 500 µL 2.5 µM GST-Importin α were added to the column, a sample from the "input" fraction was taken and the column was incubated for 2 h on a rotator. The samples from the "input" fraction were collected to validate that equal amounts of protein were added during the pull-down assay. Unbound protein was removed by three washing steps with PBST followed by centrifugation. 500 µL 2.2 µM inactive Taspase $1_{D233A/T234A}$-His were pre-incubated with the respective concentration of **11d/e/f** on a rotator for 1 h. The final DMSO concentration of all samples was adjusted to the highest DMSO concentration used to correct effects on the interaction that were caused by the solvent. Again, a sample for the "input" fraction was retained. The free binding sites on the column were blocked with 1 % (w/v) BSA (Carl Roth) in PBST for 30 min on a rotator. The blocking solution was removed from the column by centrifugation. Subsequently, Taspase $1_{-D233A/T234A}$-His pre-incubated with **11d** or DMSO was added to the column and incubated on a rotator for 1 h to allow binding to GST-Importin α. Unbound protein was removed by centrifugation. A sample of the "unbound" fraction was taken to validate that the compound did not elute GST-Importin α from the column. We applied three washing steps with PBST followed by centrifugation. Finally, 500 µL 1 x sample buffer[19] was added to the column and heated to 95 °C for 10 min to denature all protein on the column. Proteins were eluted by centrifugation for 2 min and analyzed using SDS-PAGE and immunoblotting.

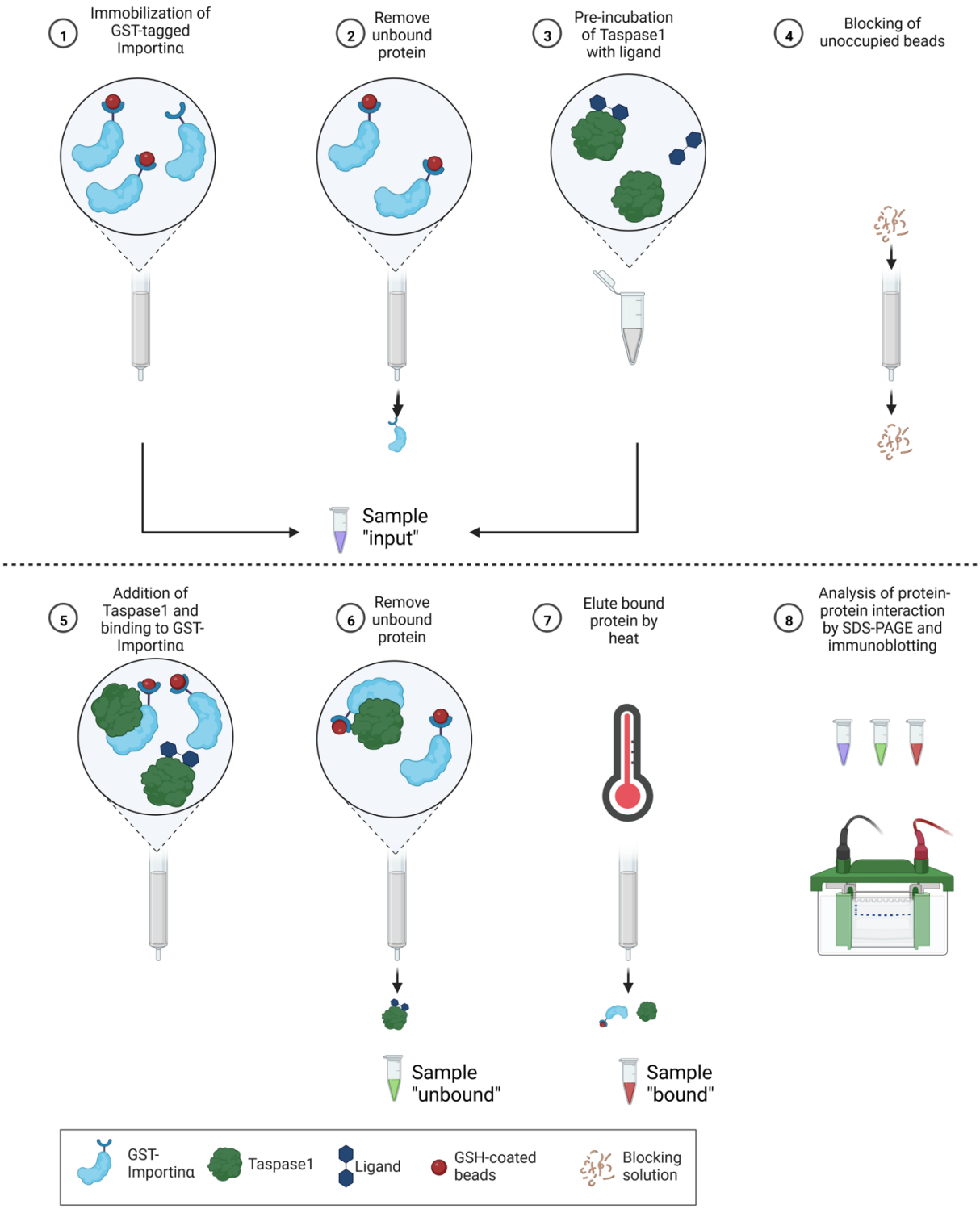

Figure S10. Schematic workflow of the pull-down assay. A spin column was used to immobilize GST-Importin α (cyan) on a Sepharose matrix coated with glutathione (1). First, GST was allowed to bind to glutathione (GSH-coated beads, dark red) with high affinity, and unbound protein was removed by centrifugation (2). Then, Taspase 1-His (dark green) was pre-incubated with ligand (dark blue) or solvent (DMSO) as indicated (3), subsequently added to the previously blocked (4) column (5), and unbound protein was again removed by centrifugation (6). Next, a buffer containing ionic detergents as well as reducing agents was applied to the column and heated to 95 °C to denature and thus dissociate all protein from the matrix (7). Finally, the proteins were separated according to their molecular weight by SDS page and analyzed by immunoblot analysis for quantification (8). Arrows indicate when the different samples “input” (violet), “unbound” (green) and “bound” (magenta) were collected. Created with BioRender.com.

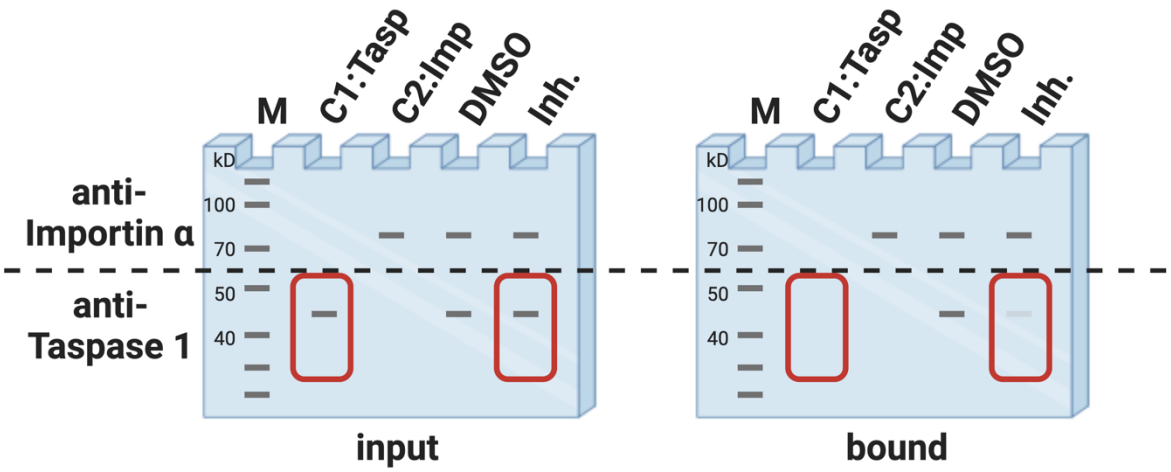

Figure S11. Schematic outcome of the pull-down assay. In the input of the pulldown assay, protein bands for Taspase 1 can be detected in the Taspase 1 control (C1) and in all treatment samples (DMSO and inhibitor), whereas protein bands for Importin α are present in the Importin α control (C2) and likewise in all treatment samples. In contrast, Taspase 1 should not be detectable in the Taspase 1 control (C1) of the bound fraction as this would indicate for unspecific binding to the column in the absence of Importin α (red box, C1). Importin α should be still detectable in the respective control (C2) in the bound fraction as it is loaded onto the column. An efficient inhibitor of the Taspase 1/Importin α interaction would significantly diminish the amount of Taspase 1 in the bound fraction (red box, Inh.). M, molecular weight marker. Created with BioRender.com.

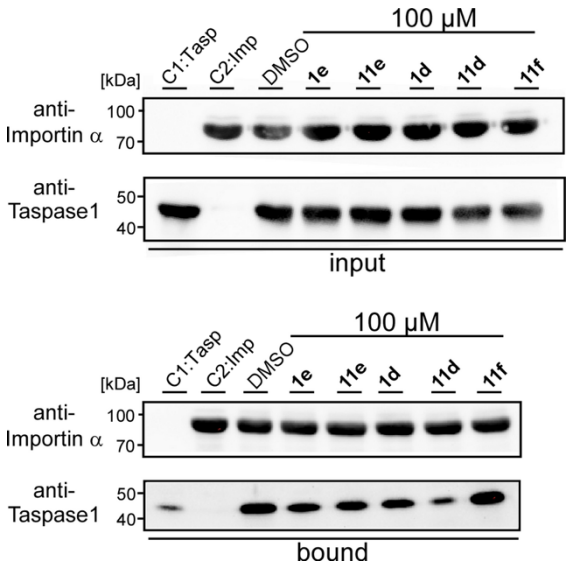

Figure S12. Pull-down assays characterize **11d** as the most promising inhibitor of the Taspase 1/Importin α interaction. Assays were performed with 100 µM of indicated ligands, one representative example is shown. Controls: Taspase 1-His (C1) or GST-Importin α (C2) alone were added to the column, and a DMSO-treated sample served as reference.

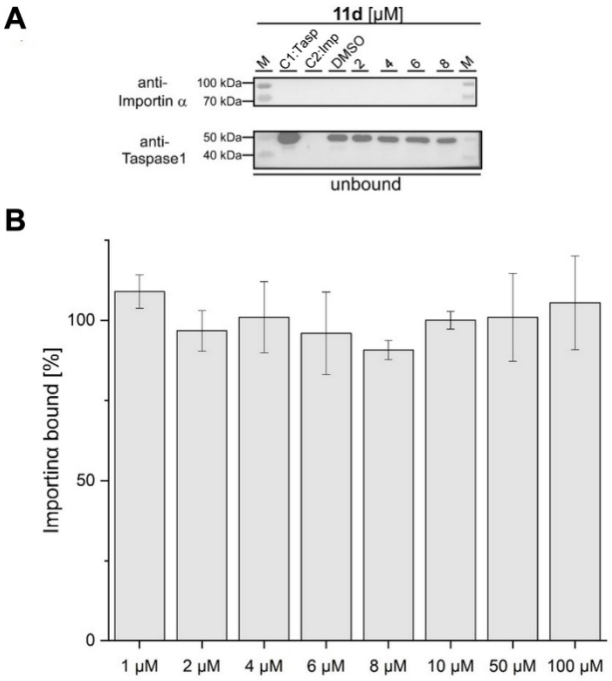

Figure S13. Immunoblot of the "unbound" fraction after incubation with Taspase 1 and **11d**. A) Binding of Importin α to the column was not affected by the ligands during the assay, while unbound Taspase 1 was removed. Chemiluminescence images were merged with colorimetric images to allow visualization of the marker (M). Controls included Taspase 1 (C1), GST-Importin α (C2) alone or a DMSO-treated control. B) Densitometric quantification of Importin α bound in the "eluted" fraction of the pull-downs shows, that Importin α-binding to the column was not affected by the compound. The results are the mean of three replicates ± standard deviation.

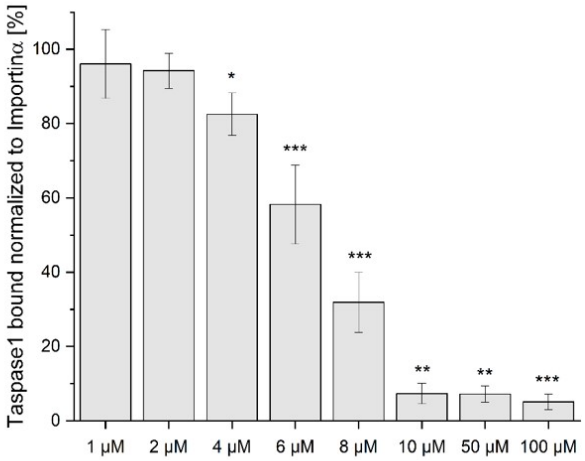

Figure S14. Densitometric quantification of the pull-down results. The results are the mean of three replicates ± standard deviation. *p<0.05; ** p<0.01; ***p<0.001.

Fluorescence anisotropy titration with full-length Taspase 1

Fluorescence anisotropy was performed using a FP-8300 fluorescence spectrometer (Jasco, Pfungstadt, Germany) with high precision cells (Hellma Analytics, Müllheim, Germany). The titration was performed in Dulbecco's Phosphate Buffered Saline (PBS, Sigma-Aldrich) and all samples were degassed with a MicroCal ThermoVac (Malvern Pananalytical, Kassel, Germany) immediately before the experiment. The concentration of the ligand **11d** was kept constant at 1 µM during the titration with the analyte Taspase $1_{D233A/T234A}$-His. We added increasing volumes (0.5 µL, 0.5 µL, 0.5 µL, 0.5 µL, 1 µL, 2 µL, 4 µL, 8 µL, 16 µL, 32 µL, 64 µL) of a solution consisting of 20 µM protein and 1 µM **11d** to 60 µL 1 µM **11d** at 25 °C. After each titration step, the sample was properly mixed, the change in fluorescence anisotropy measured five times (λ_{exc} 380 nm, λ_{em} 400 nm) and the results averaged. The data was collected with the software Spectra Manager™ with data points representing the mean of three replicates ± standard deviation. Subsequently, the data was fit using the following quadratic binding equation for a one-site specific binding model (Graph Pad Prism 5). The K_D is given as fit ± standard error.

$$r = r_0 + \frac{r_{max} * (F + x + K_D) - \sqrt{(F + x + K_D)^2 - 4 * x * F}}{2 * F}$$

r = anisotropy, r_0 = anisotropy in the absence of protein, r_{max} = maximum anisotropy, F = fluorophore concentration, x = protein concentration, K_D = dissociation constant

For the determination of the stoichiometry, we titrated higher concentrations of Taspase 1. The data was fit using the following equation:

$$Y = F_0 + F *$$

A = concentration analyte (**11d**), x = concentration titrant (Taspase 1), F_0 = anisotropy without titrant, F = amplitude, K_D = dissociation constant, n = stoichiometry factor c(analyte)/c(titrant)

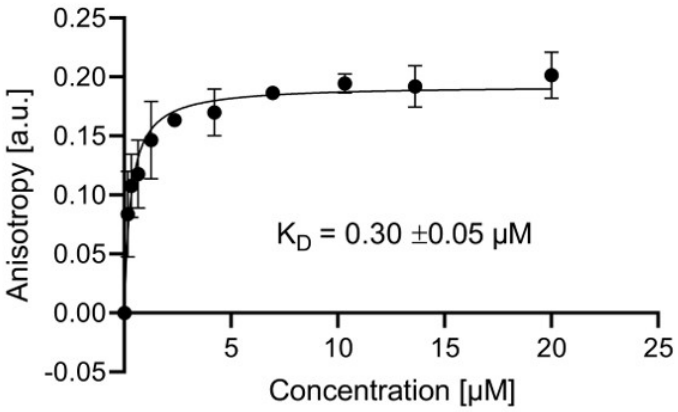

Figure S15. Fluorescence anisotropy to determine the binding affinity of **11d** for Taspase $1_{D233A/T234A}$-His. The results are the mean of three replicates ± standard deviation, K_D is given as fit ± standard error.

Fluorescence titration with the Taspase 1 loop

The Taspase 1 loop with an N-terminal FAM-label was synthesized by GeneCust (Sequence: FAM-SCPPNIMTTRFSLAAF**KRNKRK**LELAERVDTDFMQL**KKRR**QSSEKENDSGTLD, NLS highlighted). In a 96 well-plate, the Taspase 1 loop peptide was mixed with respective concentrations of **11d**. Untreated controls were treated with respective concentrations of DMSO. While the loop was used at a fixed concentration of 1 µM, we still performed one dilution control per concentration to avoid potential dilution artefacts. Fluorescence was observed using the Promega GloMax (Promega) equipped with the blue filter set (Excitation 490 nm, Emission 510 - 570 nm). The samples were corrected for potential dilution effects and normalized to untreated controls. To exclude the possibility of the compound binding to the label, we used FAM without peptide as a negative control for the highest compound concentration. The data points are the mean of three replicates ± standard deviation. The data was fit using the following quadratic binding equation for a one-site specific binding model (Graph Pad Prism 5). The K_D is given as fit ± standard error.

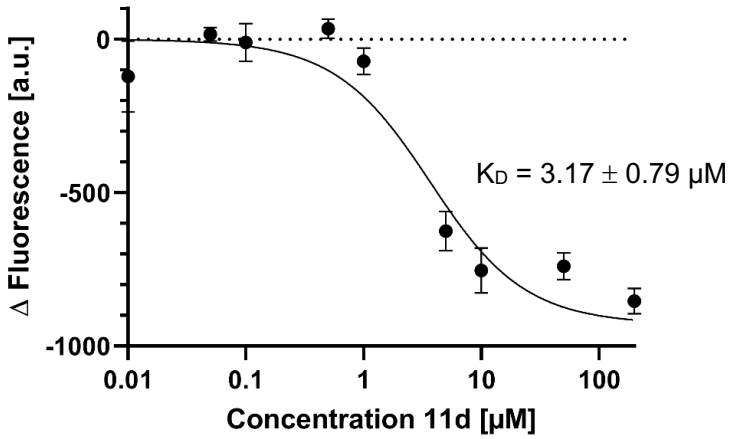

Figure S16. Fluorescence titration of Taspase 1 loop with **11d**. 1 µM FAM-labeled Taspase 1 loop. The results are the mean of triplicates ± standard deviation, the K_D is given as fit ± standard error.

Protein NMR spectroscopy

NMR experiments were recorded at 25 °C on a Bruker 700 MHz Avance Ultrashield NMR spectrometer (Bruker, Germany) equipped with a 5 mm TCI $^{1}H/^{13}C/^{15}N/D$ cryoprobe with z-gradient. Spectra were processed with Topspin 3.5 and analyzed in CARA.[22]

^{15}N-Taspase 1 $loop_{178-233}$ (274 µM) in NMR buffer (1.5 mM KH_2PO_4, 8.9 mM Na_2HPO_4, 136.9 mM NaCl, 2.7 mM KCl, pH 6.5) containing 5 % D_2O was titrated with a 5 mM stock of **11d** in DMSO-d6, yielding a final ligand concentration of 300 µM in the presence of at most 6 % DMSO-d6. $^{1}H,^{15}N$-HSQC spectra were recorded for each titration step. To account for slight shifting of signals due to the presence of DMSO, a control titration with the corresponding volumes of DMSO-d6 without ligand was performed. The relative signal intensities I/I_0 were evaluated,[23] where I represents the signal intensity in the presence of ligand and I_0 the intensity in the DMSO-only reference spectrum. A more than average decrease in intensity also indicates ligand binding due to intermediate exchange kinetics. The amide chemical shift perturbations did not yield useful data because signals already disappeared at small ligand concentrations and thus did not allow tracking of their positions.

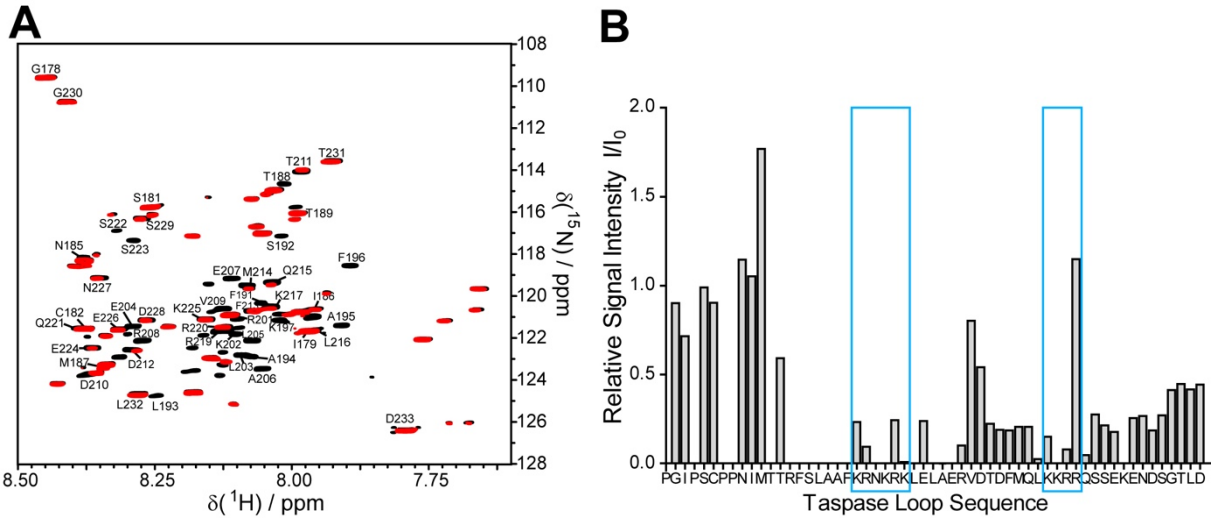

Figure S17. Protein NMR spectroscopy. A) ^{1}H-^{15}N-BEST-TROSY-HSQC spectra of 300 µM ^{15}N-labeled Taspase 1 $loop_{178-233}$ with (red) and without (black) 300 µM **11d**. B) The relative signal intensities show a decrease within Taspase 1's bipartite NLS (blue frame) indicating ligand binding within this region.

Colorimetric cleavage assay

This novel assay utilized a recombinant GST-$MLL_{2700-2850}$-GFP-His with the CS2 cleavage site as a Taspase 1 substrate. If not stated otherwise, all proteins were prepared in Taspase 1 kinetic buffer (10 % sucrose, 50 µM NaH_2PO_4, pH 7.4). Taspase 1 was thawed for 5 min and different aliquots pooled to assure equal protein activity. Taspase 1 and respective concentrations of ligand or DMSO were added into reaction tubes. One negative control contained buffer instead of Taspase 1. In intervals of 15 s the substrate was added to the reaction tubes and the mixture incubated at 37 °C for 90 min. In intervals of 15 s the reaction was stopped by adding 5x sample buffer and heating to 95 °C. The proteins were analyzed using SDS-PAGE and visualized using Coomassie stain solution. The gels were covered with Coomassie staining solution and heated in the microwave at 800 W for 15 s. After 45 min incubation on a rocking shaker the staining solution was removed, and the gel was covered in destaining solution and destained overnight on a rocking shaker. For imaging we used a Chemidoc Imaging System (BioRad). Densitometric quantification of the signals was performed using Fiji.[20] The background was subtracted using the rolling ball algorithm with 50 pixels. Of note, the amount of Taspase 1 used was below the detection limit of the later used Coomassie stain, allowing easier quantification of the substrate protein bands. To avoid differences in loading, we only compared the ratio between cleaved and uncleaved substrate per sample and determined the relative cleaved substrate per sample. We normalized the samples to the untreated control to determine the effect of the compound on the proteolytic activity. The data was evaluated using Origin2019 (OriginLab). To correct differences in the variance of the samples, significances were determined using the Welch-t-test.

Competitive FRET-based cleavage assay

This assay is a modified version of a procedure described in literature.[24] The peptide used as a substrate was synthesized by Bachem. The N-terminal fluorophore Tide fluor 2 was separated from the C-terminal quencher Tide 2 quencher by the peptide sequence KISQLD/GVDDGC containing a cleavage site for Taspase 1 (cleavage site indicated). HeLa Kyoto cells were lysed using sonication and a standard RIPA buffer. Cell debris was removed by centrifugation at 11000 x G and the supernatant was transferred to a new reaction tube. 8 µM substrate, respective concentrations of lysate and 2 µM **11d** were mixed in a 96 well plate. We included a negative control without recombinant Taspase 1 to correct for endogenous Taspase 1 in the lysate and possible fluorescence introduced by the compound. Taspase 1-His was thawed for 5 min and added to the mix. Fluorescence was observed using the Promega GloMax (Promega) equipped with the blue filter set (Excitation 490 nm, Emission 510-570 nm). Fluorescence was detected after the intervals given (10 x 1 min, 10 x 2 min, 10 x 10 min, after 180 min total, after 210 min total). The signal in the untreated control was subtracted from the other measurements. The fluorescence given in auxiliary units was converted into µM of cleaved substrate using the following equation:

$$[S_C] = \frac{[S_T] * I_{measured} - I_{intact}}{I_{cleaved} - I_{intact}}$$

$[S_C]$ = concentration of cleaved substrate in µM; $[S_T]$ = concentration of total substrate in µM; $I_{measured}$ = observed intensity; I_{intact} = minimum intensity with no substrate cleaved; $I_{cleaved}$ = maximum intensity with all substrate cleaved.

The signal in the first 5 min was used to determine the initial velocity with linear regression. The results were normalized to DMSO-treated controls to determine the relative activity of Taspase 1 after compound treatment. The data was evaluated using Origin2019 (OriginLab). To correct differences in the variance of the samples, significances were determined using the Welch-t-test.

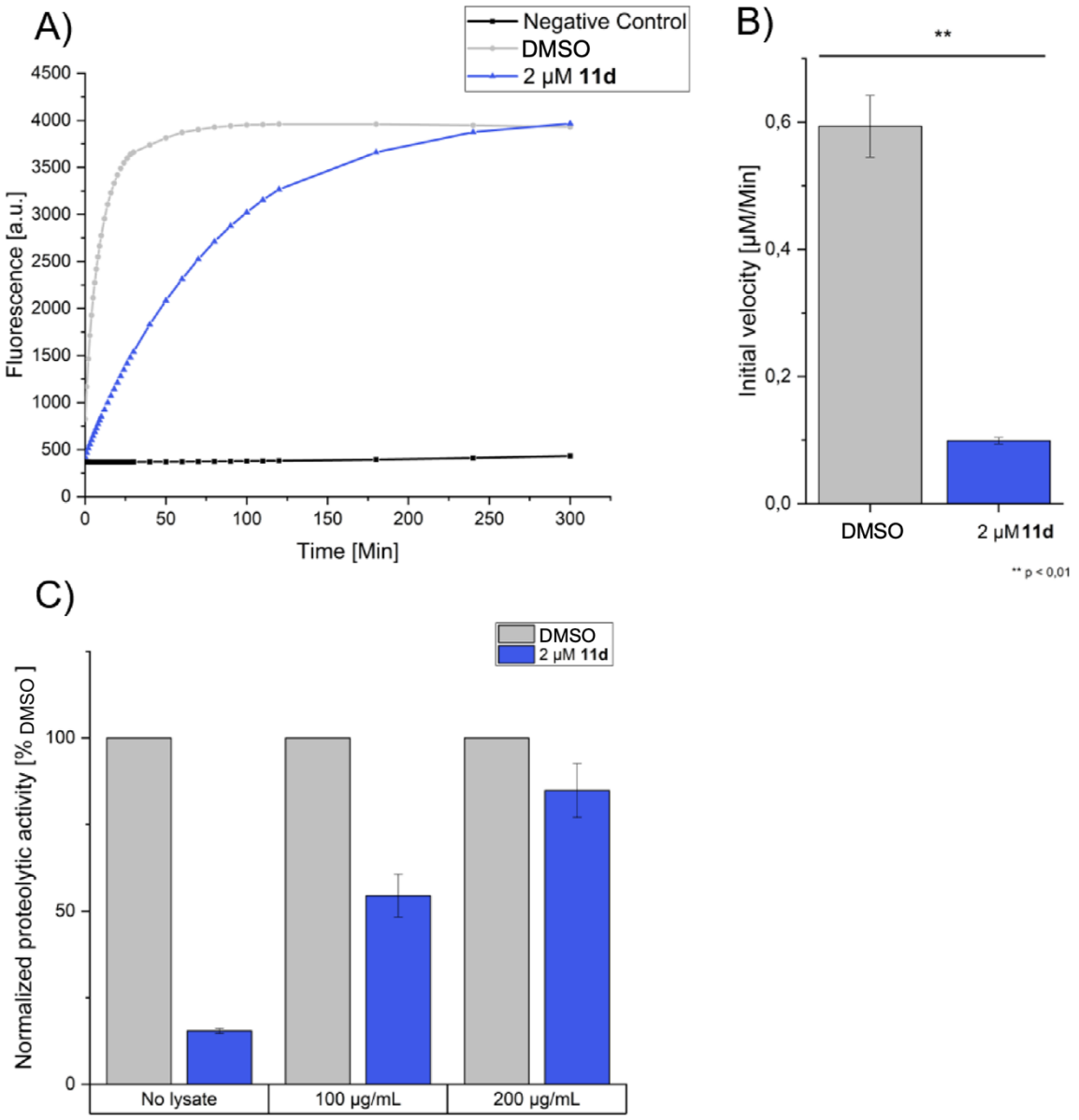

Figure S18. FRET-based cleavage assay. A) Exemplary curve showing the effect of 2 µM **11d** on Taspase 1 activity. B) Initial velocity of Taspase 1 enzymatic activity over the first 5 min is significantly decreased by the addition of 2 µM **11d**. The results are the mean of three replicates ± standard deviation. C) A competitive version of the FRET-based cleavage assay shows that **11d** still affects the proteolytic activity of Taspase 1, even if 30- or 60-fold excess of cell lysate is added.

Microscopy

Confocal laser microscopy

2 x 10^4 HeLa Kyoto cells were seeded in 200 µl Dulbecco's modified eagle medium (Thermo Fisher Scientific) in µ-Slide 8 Well (Ibidi) supplemented with 10 % (v/v) FCS (Life Technologies GmbH) and Antibiotic-Antimycotic (Life Technologies GmbH). The live cells were incubated in DMEM supplied with 50 µM **11d** or respective concentrations of DMSO for 1 h or 24 h at 37 °C and 5 % CO2. Remaining compound was removed by three washing steps with Dulbecco's phosphate-buffered saline (Sigma-Aldrich) (PBS). To subsequently allow robust and reliable measurements unaffected by the time required for image acquisition, the cells were fixed using paraformaldehyde for 20 min at room temperature followed by a washing step with PBS at indicated time points of the respective experiment. To stain the outer plasma membrane, we applied Cellbrite® green (Biotium) in PBS for 30 min at 37 °C. After that, the cells were washed with PBS three times. For microscopy, we used the "Leica TCS SP8X Falcon" (Leica). Maximum intensity projection images of the cells were generated from image stacks with "LasX" (Leica).

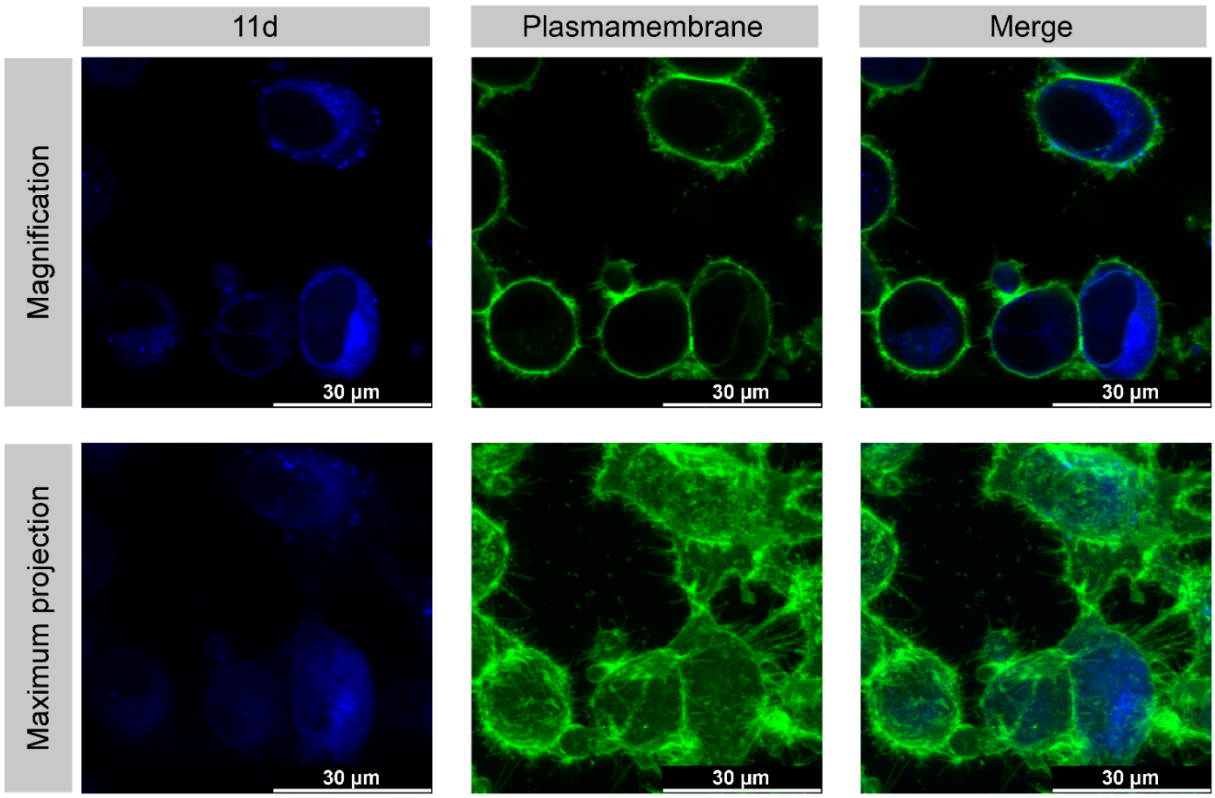

Figure S19. 11d enters living tumour cells (see also Fig. 7). Cells were incubated with 50 µM **11d** for 1 h, and the plasma membrane was stained with CellBrite® (green). Confocal microscopy detects the blue-fluorescent compound **11d** inside HeLa Kyoto cells. The same image plane as presented in the magnification (upper panel) with a maximum intensity projection is shown (lower panel), based on a stack of optical sections. Scale bars, 30 µm.

Intracellular biosensor assay

The biosensor for Taspase 1 is an established assay for intracellular Taspase 1 activity.[16] HeLa Kyoto cells were seeded to 60 % confluency in 200 µl Dulbecco's modified eagle medium (DMEM, Thermo Fisher Scientific) in µ-Slide 8 Well (Ibidi) supplemented with 10 % (v/v) FCS (Life Technologies GmbH) and Antibiotic-Antimycotic (Life Technologies GmbH). After 4 h incubation at 37 °C and 5 % CO_2 the cells were transfected with the red fluorescent biosensor $TASP_{BS}$ (pC3-TS-Cl2+$_R$) 4 h after seeding using Lipofectamine 2000 (Invitrogen). After 4 h medium was exchanged for DMEM supplemented with 50 µM **11d**. The control was treated with respective concentrations of DMSO. 30 h after transfection, equaling 26 h of compound treatment, the cells were washed three times with Dulbecco's phosphate-buffered saline (PBS, Sigma-Aldrich). To exclude the formal possibility of unspecific interference with import of the biosensor itself, we additionally treated the cells with 20 nM of the export inhibitor LMB (Sigma Aldrich) for another 1 or 3 h. Before inspection on a "Leica TCS SP8X Falcon" (Leica) confocal microscope, the cells were fixed with paraformaldehyde for 20 min at room temperature and washed with PBS three times. Images were randomized using the Fiji macro "Filename randomizer".[21] Based on the intensity of the $TASP_{BS}$ biosensor signal, its distribution patterns were assigned to the three categories "Predominantly nucleus", "Equally distributed" and "Predominantly cytoplasm" (Figure S20B). Of note, the category "Predominantly nucleus" also included cells with a completely nuclear localization of the biosensor, whereas no exclusively cytoplasmic localization of $TASP_{BS}$ could be detected. The number of cells showing each distribution pattern was normalized to the total number of cells evaluated. For each sample the distribution pattern of at least 130 cells was evaluated. The results are the mean of three replicates ± standard deviation. The data was evaluated using Origin2019 (OriginLab). Significances were determined by Welch-t-test to correct differences in the variance of the samples. To determine the inhibitory effect of **11d**, the ratio of the mean percentage of cells in the category "Predominantly cytoplasm" (P_C) vs. "(Predominately) nucleus" (P_N) was calculated and set to 1 for the DSMO control.

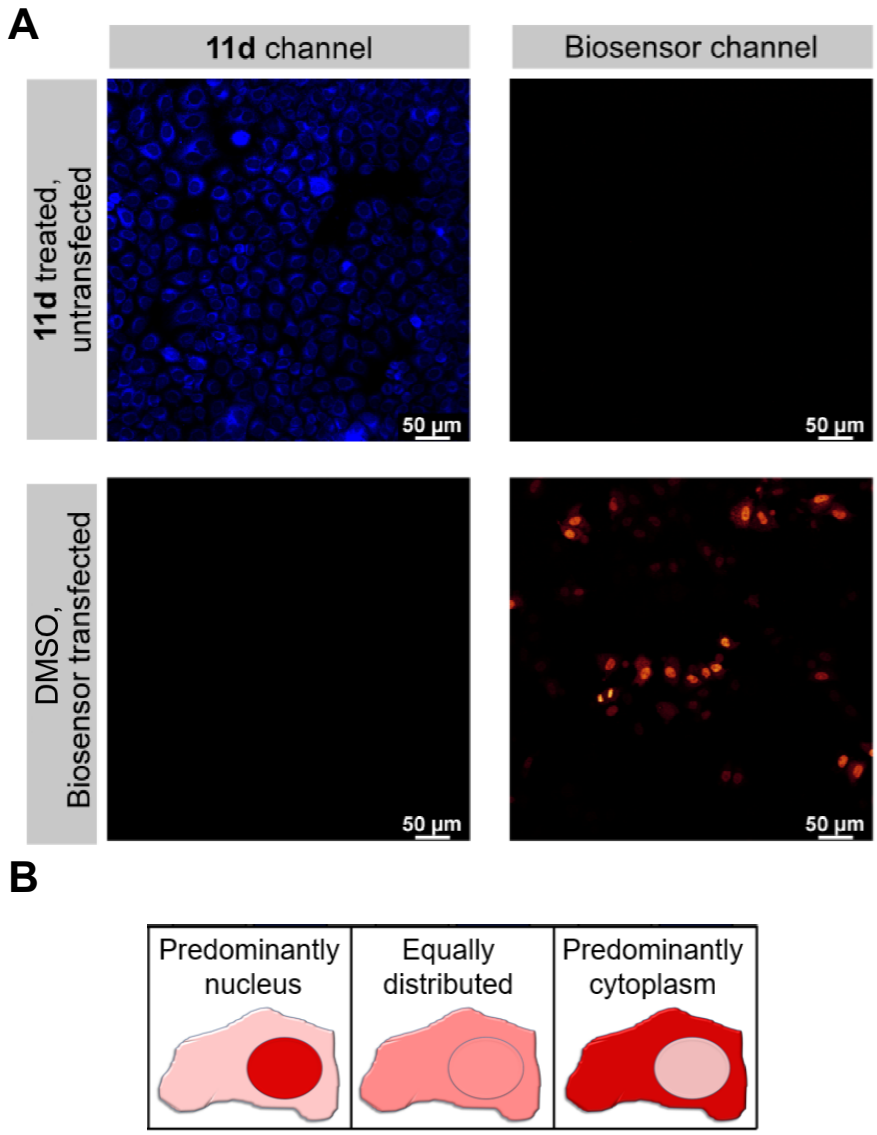

Figure S20. Optimization of the confocal laser scanning microscope setup. A) Neither is the compound **11d** detectable in the $TASP_{BS}$ biosensor channel, nor is the biosensor visible in the **11d** channel in this microscopy setup. B) Assignment of the biosensors' distribution patterns into different categories based on $TASP_{BS}$ fluorescence intensity in the different cellular compartments.

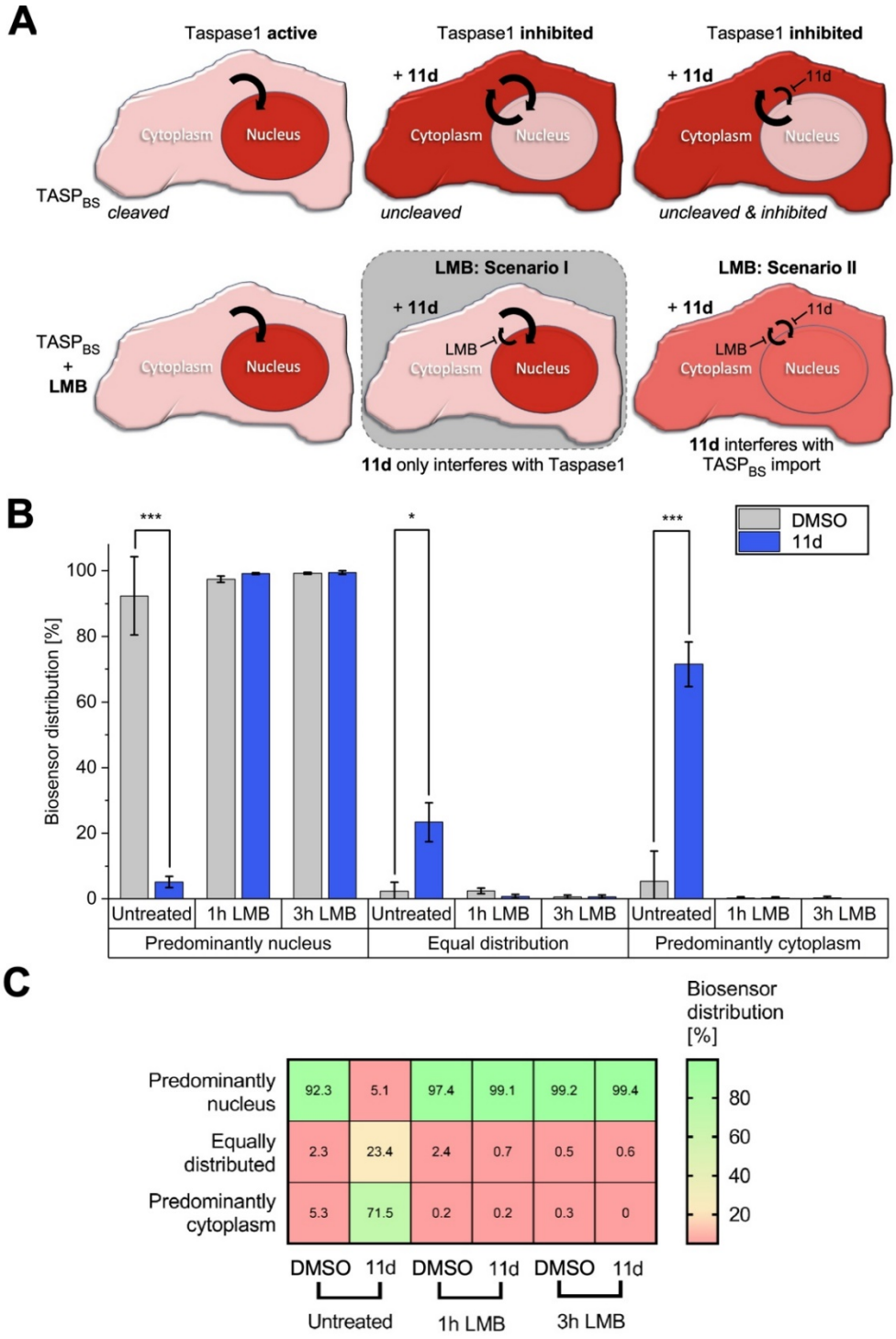

Figure S21. Specificity of the cellular biosensor for Taspase 1 inhibition by **11d**. A) Schematic of the expected distribution of the biosensor in the Leptomycin B (LMB) control setup. Active Taspase1 cleaves the dominant NES from the biosensor resulting in its nuclear accumulation that is not altered by LMB export inhibition (left panel). When Taspase1 is inhibited by **11d**, the uncleaved biosensor shuttles between nucleus and cytoplasm and is predominantly cytoplasmic (middle and right panel; see also Fig. 8). In this setting, treatment with LMB allows to discriminate between a situation where 11d is only affecting Taspase 1 activity (middle panel, scenario I) or also interferes with import of the biosensor TASP$_{BS}$ (right panel, scenario II). Whereas in scenario I the uncleaved biosensor accumulates in the nucleus after export inhibition (middle panel, highlighted in grey), import interference by **11d** in scenario II would counteract LMB-mediated export inhibition and result in a cytoplasmic shift of the biosensor (right panel). B) Quantification of TASP$_{BS}$'s intracellular localization in TASP$_{BS}$-expressing HeLa Kyoto cells, treated with 50 µM **11d** or DMSO control for 26 h, and successively incubated with LMB for 1 or 3 h before fixation. Microscopic images of at least 130 cells were acquired and randomized for localization assignment (see SI, Table S5). Results are the mean of triplicates ± standard deviation (*$p < 0.05$; ***$p < 0.001$).

Table S5. Raw data of the intracellular biosensor distribution.

Treatment	**Replicate**	**Intracellular location of the biosensor**			**Cells in total**	
		Predominantly nucleus (P_N)	Equal distribution	Predominantly cytoplasm (P_C)		Ratio P_C/P_N
DMSO	#1	187 (98.4 %)	3 (1.6 %)	0 (0 %)	190	
DMSO	#2	103 (78.6 %)	7 (5.3 %)	21 (16 %)	131	
DMSO	#3	179 (100 %)	0 (0 %)	0 (0 %)	179	
	mean [%]	92.3 %	2.3 %	5.3 %		0.0579
50 µM **11d**	#1	7 (3.9 %)	30 (16.8 %)	142 (79.3 %)	179	
50 µM **11d**	#2	7 (4.4 %)	45 (28.1 %)	108 (67.5 %)	160	
50 µM **11d**	#3	9 (7.1 %)	32 (25.2 %)	86 (67.7 %)	127	
	mean [%]	5.1 %	23.4 %	71.5 %		13.957
Inhibitory effect (fold change)						241.2
20 nM **LMB** (1h)						
DMSO	#1	182 (96.8 %)	6 (3.2 %)	0 (0 %)	188	
DMSO	#2	151 (96.8 %)	4 (2.6 %)	1 (0.6 %)	156	
DMSO	#3	131 (98.5 %)	2 (1.5 %)	0 (0 %)	133	
	mean [%]	97.4 %	2.4 %	0.2 %		0.0022
50 µM **11d**	#1	203 (99 %)	2 (1 %)	0 (0 %)	205	
50 µM **11d**	#2	176 (98.9 %)	2 (1.1 %)	0 (0 %)	178	
50 µM **11d**	#3	164 (99.4 %)	0 (0 %)	1 (0.6 %)	165	
	mean [%]	99.1 %	0.7 %	0.2 %		0.0020
Inhibitory effect (fold change)						0.93
20 nM **LMB** (3h)						
DMSO	#1	185 (99.5 %)	1 (0.5 %)	0 (0 %)	186	
DMSO	#2	131 (99.2 %)	0 (0 %)	1 (0.8 %)	132	
DMSO	#3	178 (98.9 %)	2 (1.1 %)	0 (0 %)	180	
	mean [%]	99.2 %	0.6 %	0.3 %		0.0025
50 µM **11d**	#1	183 (98.9 %)	2 (1.1 %)	0 (0 %)	185	
50 µM **11d**	#2	155 (99.4 %)	1 (0.6 %)	0 (0 %)	156	
50 µM **11d**	#3	154 (100 %)	0 (0 %)	0 (0 %)	154	
	mean [%]	99.4 %	0.6 %	0 %		0
Inhibitory effect (fold change)						0

Cell viability assay

1 x 10^4 HeLa Kyoto cells were seeded in 100 µL DMEM (Thermo Fisher Scientific) supplemented with 10 % (v/v) FCS (Life Technologies GmbH) and Antibiotic-Antimycotic (Life Technologies GmbH) into a Corning 96 Well microplate (Sigma Aldrich) and incubated at 37 °C and 5 % CO_2 over night to achieve adherence. The next day, the medium was exchanged for fresh medium with the respective compound concentrations and 1 % DMSO. After 72 h incubation in compound-supplied medium at 37 °C and 5 % CO_2 20 µL Cell Titer Aqueous One (Promega) were added and after 30 Min the absorbance at 490 nm was measured utilizing a Promega Glow Max (Promega) to determine cell viability. The results were normalized to untreated controls and are the mean of three replicates ± standard deviation.

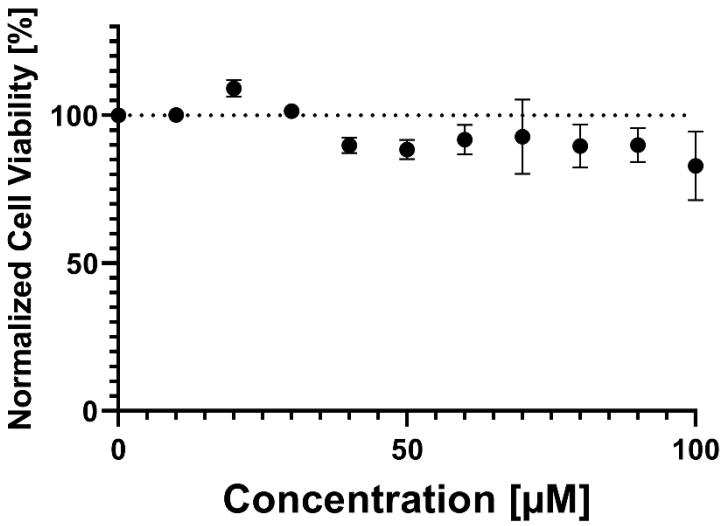

Figure S22. Cell viability assay. Cell viability of HeLa Kyoto cells is not affected by **11d** even after 72 h of incubation. The results are the mean of triplicates ± standard deviation.

Software

The atomistic models of the ligands were created in ChemDraw prime 16.0 (PerkinElmer). Structures for modelling were obtained using Maestro Schrodinger V.3.0.,[4] OpenBabel V.3.1.0.[5] or PDB2PQR web service v3.1.0 with the Amber force field option.[8] Modelling data was visualized by VMD (version 1.9.4).[25] Images of Western blots and Coomassie gels were acquired by the Chemidoc Imaging System (BioRad), quantified by densitometric analysis with Fiji,[21] and the data was evaluated using Origin 2019 (OriginLab). For data acquisition of fluorescence titrations, was the software Spectra Manager™ II (Jasco) or GloMax (Promega) supplied with the instrument were used, and data was plotted with GraphPad Prism 8 (version 8.4.1). Cleavage assay data was evaluated using Origin 2019 (OriginLab). NMR data were collected using Topspin 3.5 (Bruker) using the NMRlib 2.0 pulse sequence tools library from IBS (Grenoble, France) available at http://www.ibs.fr/research/scientific-output/software/pulse-sequence-tools/. NMR spectra were processed with Topspin 3.5 (Bruker) and analyzed in CARA (version 1.9.1.7; http://cara.nmr.ch). Relative signal intensities were calculated from the raw chemical shift data and peak intensities using Excel 2016 (Microsoft) and plotted with GraphPad Prism 5.0. Microscopy data was generated by "LasX" (Leica), and images were randomized using the Fiji macro "Filename randomizer".[21] Figure panels were assembled in CanvasDraw 6.0 (ACDsee) or PowerPoint 2016 (Microsoft). Selected figures were created with Biorender.com as indicated.

References

1. F. Octa-Smolin, M. Thiele, R. Yadav, A. Platzek, G. H. Clever and J. Niemeyer, *Org. Lett.*, 2018, **20**, 6153-6156.
2. F. Octa-Smolin, F. van der Vight, R. Yadav, J. Bhangu, K. Soloviova, C. Wolper, C. G. Daniliuc, C. A. Strassert, H. Somnitz, G. Jansen and J. Niemeyer, *J. Org. Chem.*, 2018, **83**, 14568-14587.
3. R. Yadav, C. Kwamen and J. Niemeyer, *Isr. J. Chem.*, 2021, **61**.
4. S. Maestro, LCC, *Journal*, 2021.
5. N. M. O'Boyle, M. Banck, C. A. James, C. Morley, T. Vandermeersch and G. R. Hutchison, *J. Cheminformatics*, 2011, **3**, 33.
6. W. D. Kumler and J. J. Eiler, *J. Am. Chem. Soc.*, 1943, **65**, 2355–2361.
7. J. van den Boom, F. Trusch, L. Hoppstock, C. Beuck and P. Bayer, *PLoS One*, 2016, **11**, e0151431.
8. T. J. Dolinsky, J. E. Nielsen, J. A. McCammon and N. A. Baker, *Nucleic Acids Res.*, 2004, **32**, W665-667.
9. J.-N. Grad, A. Gigante, C. Wilms, J. N. Dybowski, L. Ohl, C. Ottmann, C. Schmuck and D. Hoffmann, *J. Chem. Inf. Model.*, 2018, **58**, 315–327.
10. N. Rafieiolhosseini, M. Killa, N. Tötsch, J.-N. Grad, A. Höing, C. Ottmann, S. K. Knauer, J. Voskuhl and D. Hoffmann, *Beilstein J. Org. Chem.* 2022, **18***,* 1322–1331..
11. A. Milchev and K. Binder, *Macromolecules*, 1996, **29**, 343-354.
12. P. T. Underhill and P. S. Doyle, *J. Non-Newton. Fluid Mech.*, 2004, **122**, 3–31.
13. B. Liu, J. Wang, X. Fan, Y. Kong and H. Gao, *J. Comput. Phys.*, 2008, **227**, 2794–2807.
14. C. Bier, R. Hecht, L. Kunst, S. Scheiding, D. Wunsch, D. Goesswein, G. Schneider, O. H. Kramer, S. K. Knauer and R. H. Stauber, *PLoS One*, 2012, **7**, e34142.
15. J. van den Boom, A. Hensel, F. Trusch, A. Matena, S. Siemer, D. Guel, D. Docter, A. Höing, P. Bayer, R. H. Stauber and S. K. Knauer, *Nanoscale*, 2020, **12**, 19093-19103..
16. S. K. Knauer, V. Fetz, J. Rabenstein, S. Friedl, B. Hofmann, S. Sabiani, E. Schröder, L. Kunst, E. Proschak, E. Thines, T. Kindler, G. Schneider, R. Marschalek, R. H. Stauber and C. Bier, *PLoS One*, 2011, **6**.
17. P. Pasch, A. Höing, S. Ueclue, M. Killa, J. Voskuhl, S. K. Knauer and L. Hartmann, *Chem. Commun.*, 2021, **57**, 3091–3094.
18. D. Y. Chen, Y. Lee, B. A. van Tine, A. C. Searleman, T. D. Westergard, H. Liu, H.-C. Tu, S. Takeda, Y. Dong, D. R. Piwnica-Worms, K. J. Oh, S. J. Korsmeyer, A. Hermone, R. Gussio, R. H. Shoemaker, E. H.-Y. Cheng and J. J.-D. Hsieh, *Cancer Res.*, 2012, **72**, 736–746.
19. U. K. Laemmli, *Nature*, 1970, **227**, 680-685.
20. H. Towbin, T. Staehelin and J. Gordon, *Proc. Natl. Acad. Sci. U.S.A.*, 1979, **76**, 4350–4354.
21. J. Schindelin, I. Arganda-Carreras, E. Frise, V. Kaynig, M. Longair, T. Pietzsch, S. Preibisch, C. Rueden, S. Saalfeld, B. Schmid, J.-Y. Tinevez, D. J. White, V. Hartenstein, K. Eliceiri, P. Tomancak and A. Cardona, *Nat. Methods*, 2012, **9**, 676–682.
22. R. L. J. Keller, DOI: 10.3929/ethz-a-005068942, ETH Zurich, 2005.
23. P. Bayer, A. Matena and C. Beuck, *Beilstein J. Org. Chem.*, 2020, **16**, 2505–2522.
24. J. J.-D. Hsieh, E. H.-Y. Cheng and S. J. Korsmeyer, *Cell*, 2003, **115**, 293–303.
25. W. Humphrey, A. Dalke and K. Schulten, *J. Mol. Graphics*, 1996, **14**, 33-38, 27-38.